NUKLEONIKA 2015;60(1):51–55
doi: 10.1515/nuka-2015-0014

ORIGINAL PAPER

DE GRUYTER
OPEN

Mössbauer spectroscopy of reduced forms of a Fe-tetraphenylporphyrine complex

Tomasz Kaczmarzyk, Iwona Rutkowska, Kazimierz Dziliński

Abstract. Molecular and electronic structure changes during successive reduction of a Fe-tetraphenylporphyrin chloride [Fe(III)(TPP):Cl] complex are reported on the basis of Mössbauer spectroscopy and DFT calculations. It is established that the attachment of additional electrons to a neutral Fe(III)(TPP):Cl molecule leads to significant shortening of Fe-N distances at the first stage of the reduction Fe(III)(TPP):Cl → Fe(II)(TPP) and lengthening of these bonds at the second stage Fe(II)(TPP) → Fe(I)(TPP). Changes of other bond lengths of the porphyrin ring also appear but in less degree. Interaction of Fe(II) and Fe(I)(TPP) with tetrahydrofuran (THF) solvent is considered. Electron configuration of Fe(II)(TPP) corresponds to intermediate-spin (S = 1) state and in the case of Fe(I)(TPP) low-spin state (S = ½) is observed. Electron density distribution in Fe(II)- and Fe(I)(TPP) complexes, in association with Mössbauer data, is analyzed. Good correlation between experimental and theoretical results was obtained.

Key words: DFT calculations • electronic structure • iron-(tetraphenyl)porphyrin • Mössbauer spectroscopy • reduction process

T. Kaczmarzyk✉, I. Rutkowska, K. Dziliński
Institute of Physics,
Częstochowa University of Technology,
19 Armii Krajowej Ave., 42-200 Częstochowa, Poland,
Tel.: +48 34 325 0177, Fax: +48 34 325 0975,
E-mail: kcz@wip.pcz.pl

Received: 18 June 2014
Accepted: 15 November 2014

Introduction

Iron porphyrins are a class of biologically important macromolecules which perform many distinctive functions. They take part in reversible oxygen transport, reversible electron transfer in cytochromes and they are involved in irreversible transformations of substrates in peroxidatases [1]. Iron porphyrins are also interesting objects for coordination chemistry because of a variety of oxidation and spin states of the central Fe atom which can be coordinated with the porphyrin ring and different axial ligands. Central position of the iron atom in tetrapyrrole structures corresponds to its significant effect on chemical and physical properties of these complexes. Electron configuration at the Fe atom is sensitive to molecular structure of the surrounding ligands:porphyrin and axial [2]. Apart from the biological aspects, the molecular structure and physical properties of iron porphyrins promote these complexes for application in such contemporary technologies as non-linear optics, molecular semiconductors, liquid crystals, and so on [3]. Reduced forms of iron porphyrins play an essential role as intermediate products in the reduction–oxidation bioprocesses which modulate the course of reactions running with participation of the electron transfer. The reduction process of iron porphyrins runs in a more complex way in comparison, for example, with the Mg- or Zn-porphyrins [4], because additional electrons, joined to an iron porphyrin molecule can occupy *d*-orbitals of the

Fe-ion, π-orbitals of the porphyrin ligand or both if the metal and ligand orbitals overlap [5]. Charge transfer between *d*- and π-ligand orbitals can be realized by electronic iron-to-macrocycle back-bonding and it can generate π-anion-radical character of the porphyrin ligand in reduction products. It was also established for two-electron-reduced octaethylporphyrin and tetraphenylporphyrin iron complexes that the stronger or weaker π-anion-radical character of the porphyrin ligand depends significantly on electron-withdrawing substituents on the macrocycle [6].

Mössbauer spectroscopic characteristics and density functional theory (DFT) calculations considered in this paper concern products obtained at the first two reduction steps of a chloride Fe(III)-tetraphenylporphyrin [Fe(III)(TPP):Cl] complex. At the first stage of the reduction process, ferrous divalent Fe(II)(TPP) complexes occurred and at the second stage the univalent Fe(I)(TPP) were obtained. The divalent Fe(II)(TPP) complex has been investigated experimentally [7–9] and theoretically [10–13]. This complex has two conformations in solid state: ruffled [7, 9] and saddled [8]. It is not clear what causes the former and the latter conformations. To our knowledge, Fe(I)(TPP) complex has not been investigated by Mössbauer experimental technique. Theoretical quadrupole splitting (QS) values have not been calculated for each oxidation state of the Fe(TPP) complex so far.

Experimental and calculation procedures

Fe(III)(TPP):Cl compound was purchased from Sigma Aldrich Chemical Co. and used as a reagent of commercial quality. Tetrahydrofuran (THF) solvent was carefully degassed by freeze-throw cycles with the use of a metallic potassium and sodium alloy. The reduction process was performed using the chemical method by contact of THF solution with metallic sodium. Because reduction products are air sensitive, the reaction was carried out on a vacuum line (10^{-2} Pa), inside a special cuvette which contained a vessel where reduction reaction was carried out, cells for electronic absorption spectra and Mössbauer measurements. The course of the reduction reaction was controlled by detection of electronic absorption spectra at each stage of the reduction. Mössbauer spectra of powdered unenriched samples were recorded in horizontal transmission geometry using a constant acceleration spectrometer. The source ^{57}Co(Rh) and samples were kept at room temperature. A metallic iron foil absorber (α-Fe) was used to calibrate the velocity scale, and zero velocity was taken as the centroid of its room temperature Mössbauer spectrum. The samples for Mössbauer measurements were prepared as powder layers obtained after evaporation of the THF solvent. Not all THF molecules were removed from the layers containing Fe(II)- and Fe(I)(TPP) complexes because solvent molecules are weakly bonded to Fe-ions at 5th and 6th coordination positions as axial ligands [14, 15]. Heating of the layers at about 450 K under vacuum causes breaking away of THF molecules from iron ions of porphyrin rings. THF solvent was not removed completely from the layers because such 'dry' layers destroy and it is not possible to perform Mössbauer measurements if samples have to be mounted in vertical position. So, the Mössbauer spectra were recorded for two types of complexes: (a) pure Fe(TPP):$(THF)_2$, and (b) the mixture Fe(TPP):$(THF)_2$ + Fe(TPP). Pure Fe(II)(TPP) and Fe(I)(TPP) products of the reduction reaction (without solvent molecules) are marked as 'dry' complexes. The layers contained about 4×10^{-4} g/cm^2 of ^{57}Fe. The parameters of Mössbauer spectra were found by fitting the experimental spectra to Lorentzian lines using the NORMOS program package as done previously [16]. DFT calculations of Mössbauer parameters were carried out using the Amsterdam Density Functional (ADF) program package [8]. Molecular geometries of the Fe(II)(TPP) and Fe(I)(TPP) complexes were optimized to the energy minimum and next used for calculations. THF molecules of the solvent were omitted in the theoretical study because of some problems with convergence processes during calculations. It is important to use the same basis set, same exchange correlation functional, and same integration accuracy, if results of calculations of different molecules are to be compared. In our case, all the calculations were done with OLYP functional (Hady exchange and Lee–Young–Parr correlation potentials) and TZP (triple dzeta plus polarization) Slater type orbitals as basic functions, including the scalar relativistic ZORA treatment [8].

Results and discussion

Mössbauer spectrum of the trivalent chloride Fe(III)(TPP):Cl complex, which is a substrate of the reduction reaction, is shown in Fig. 1. The shape of this spectrum and its parameters are typical for the high spin state (S = 5/2) of iron porphyrins [17]. Although, it looks like single-line pattern, detailed analysis indicates asymmetrical doublet. To describe quantitatively the asymmetry in the Mössbauer spectra we have introduced an asymmetry parameter W_{21} which is equal to the linewidth ratio of

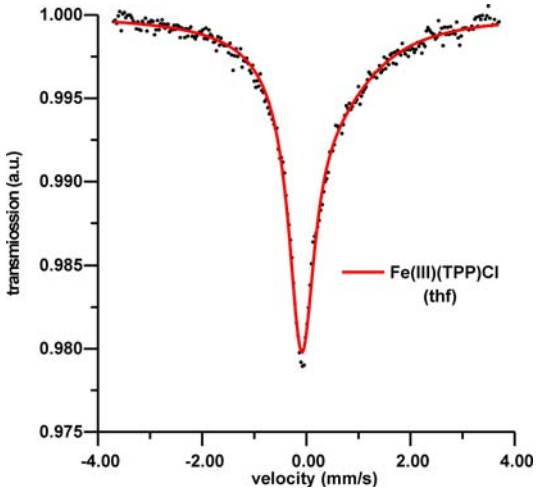

Fig. 1. Mössbauer spectrum of the substrate complex of the reduction reaction.

Table 1. Experimental Mössbauer parameters of the complexes studied

Compound	Fe(III)(TPP):Cl	Fe(II)(TPP)		Fe(I)(TPP)	
Solvent/Dry	THF	THF	Dried	THF	Dried
QS [mm/s]	0.53	2.06	1.30	1.28	1.51
IS [mm/s]	0.18	0.72	0.38	0.28	0.22
Γ_1 [mm/s]	0.61	0.22	0.19	0.22	0.23
Γ_2 [mm/s]	2.24	0.22	0.19	0.22	0.23
W_{21}	3.67	1.00	1.00	1.00	1.00

Table 2. Theoretical values of relative energies ΔE, quadrupole splittings QS and Fe-N bond lengths $R_{Fe\text{-}N}$ for different electronic configurations of Fe(II) ions in Fe(II)(TPP) for C_{4v} symmetry

Configurations				State	Fe(II)(TPP)		
b_2/d_{xy}	e_1/d_p	a_1/d_{z2}	b_1/d_{x2-y2}		ΔE [eV]	QS [mm/s]	$R_{Fe\text{-}N}$ [Å]
2	2	2	0	$^3A_2$	0.00	1.051 (1.30)[4)]	1.973 (1.972)[3)]
2	3	1	0	$^3E(A)$	0.10 (0.07)[1)]	3.036	1.978
1	4	1	0	$^3B_2$	0.29	2.309	1.986
1	3	2	0	$^3E(B)$	0.76	4.310	1.977
1	2	2	1	$^5A_1$	0.71 (0.62)[2)]	0.087	2.041
1	3	1	1	^5E[5)]	0.85	2.022 (2.06)[4)]	2.046
2	2	1	1	$^5B_1$	1.10	3.311	2.058
2	4	0	0	$^1A_1$	1.50	4.739	1.987

[1)]Experimental data from Ref. [21]. [2)]Experimental data from Ref. [22]. [3)]Experimental data from Ref. [7]. [4)]Experimental data from Table 1. [5)]Spin state symmetry from Ref. [15].

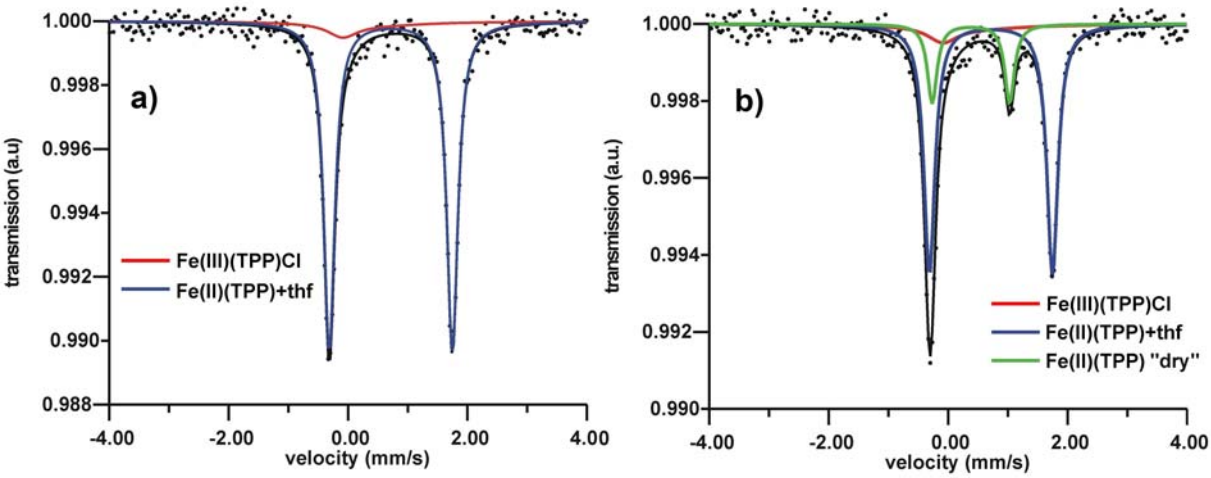

Fig. 2. Mössbauer spectra detected at the first stage of the reduction process: a) before dry, and b) after dry.

the higher energy absorption line of the doublet (the right-side line) to the lower energy absorption line (the left-side line of the doublet). This assignment is acceptable because of the equal areas under the components of the doublets. Such a kind of the asymmetry is characteristic for the temperature dependent relaxation processes [18–20] and positive sign of the V_{zz} component of electric field gradient (EFG) tensors. The positive sign of the V_{zz} indicates that Fe ion has more negative charge in the porphyrin plane than the perpendicular direction to it [17].

At the first stage of the reduction process, divalent Fe(II)-porphyrins are generated which can be diamagnetic or paramagnetic with integer spins. The recorded Mössbauer spectra of the Fe(II) reduction products are slightly asymmetrical but they can be fitted by symmetrical doublets of Fe(II)-porphyrins and the asymmetrical doublet from remains of the Fe(III)(TPP):Cl complex. Two Mössbauer spectra, recorded at this stage of the reduction process, shown in Fig. 2, correspond to the Fe(II)(TPP):$(THF)_2$ complex containing two THF molecules as axial ligands (the left one) and to the mixture Fe(II)(TPP):$(THF)_2$ + Fe(II)(TPP) (the right one). In the former case, the Fe(II) ion has electron configuration corresponding to the high spin state (S = 2) and for the pure, without THF molecules, Fe(II)(TPP) – the intermediate spin state (S = 1) is expected [14, 15]. Values of the Mössbauer parameters differ significantly for these two divalent iron porphyrins. Theoretical QS values calculated with the DFT method (Table 2) are in very good agreement with the experimental data. Very good agreement was obtained also for ionization energy (Table 3). It is widely assumed that the energy of HOMO corresponds to the ionization potential and the energy of LUMO is used to estimate the electron affinity [23].

Next stage of the reduction process leads to Fe(I)(TPP) complexes. The Mössbauer spectra show symmetrical doublets (Fig. 3). Like in the

Table 3. Theoretical values of ionization energy for different electronic configurations of Fe(II) ions in Fe(II)(TPP) with reference to the electron configuration of $(d_{xy})^2(d_{xz},d_{yz})^2(d_{z2})^2$

Configurations						Fe(II)(TPP)$^{+1}$
b_2/d_{xy}	e_1/d_π	a_1/d_{z2}	b_1/d_{x2-y2}	a_2	a_1	Ionization energy [eV]
2	2	1	0	2	2	6.01 (1st)
1	2	2	0	2	2	6.36
2	2	2	0	1	2	6.50 (6.50)[1)]
2	2	2	0	2	1	6.62

[1)]Experimental data from Ref. [24].

Table 4. Theoretical values of electron affinity energy, relative energies ΔE, quadrupole splittings QS, and Fe-N bond lengths $R_{Fe\text{-}N}$ for different electronic configurations of Fe(I) ions in Fe(I)(TPP) for C_{4v} symmetry

Configurations				Fe(II)(TPP)$^{-1}$	Fe(I)(TPP)		
b_2/d_{xy}	e_1/d_π	a_1/d_{z2}	b_1/d_{x2-y2}	Electron affinity energy [eV]	ΔE [eV]	QS [mm/s]	$R_{Fe\text{-}N}$ [Å]
2	4	1	0	−2.40	0.32	2.477	1.979
2	3	2	0	−2.08 (−1.87)[1)]	0.00	1.220 (1.28)[3)] (1.51)[3)]	1.976 (1.980)[2)]
2	3	1	1	−2.96	0.88	3.502	1.987

[1)]Experimental data from Ref. [25]. [2)]Experimental data from Ref. [26]. [3)]Experimental data from Table 1.

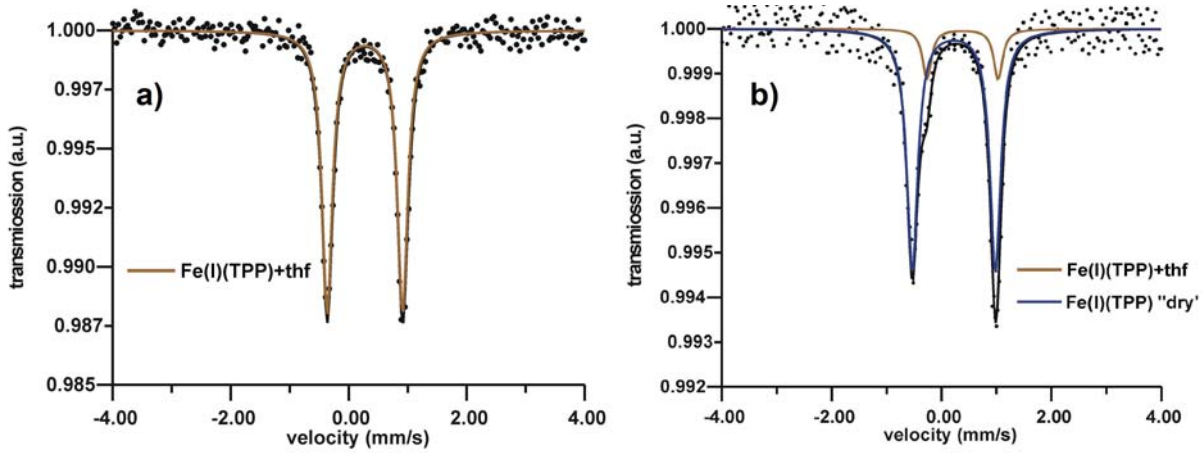

Fig. 3. Mössbauer spectra detected at the second stage of the reduction process: a) before dry, and b) after dry.

case of the divalent complex, two spectra have been analyzed. It is not clear at the moment, one or two THF molecules are joined to the Fe(I) ion. Electronic configuration indicates low-spin state (S = ½) of the Fe(I) ions. There is not much literature data for the univalent iron porphyrins, and some of the existing data is controversial. A good correlation between experimental and theoretical data was obtained also for the Fe(I)(TPP) reduction product, with respect to the quadrupole splitting (QS) and to the electron affinity energy (Table 4). It should be noted that the attachment of additional electrons to a neutral Fe(III)(TPP):Cl molecule leads to significant shortening of Fe-N distances at the first stage of the reduction Fe(III)(TPP):Cl → Fe(II)(TPP) and lengthening of these bonds at the second stage Fe(II)(TPP) → Fe(I)(TPP) (Tables 2 and 4). Changes of other bond lengths of the porphyrin ring also appear but in less degree. The ΔE values correspond to the total energy differences between the ground state and states corresponding to other electron configurations of the iron ions, considered here as excited states.

The reduction process can also run at higher stages, but detailed product determination of such a reaction is a rather difficult task and it needs further investigation.

Conclusions

Combination of experimental data with theoretical calculations is an effective approach to study electronic structure, even in the case of relatively complex systems like iron porphyrins.

We have obtained very good correlation between the experimental and theoretical results concerning the Mössbauer parameters and electronic structure of the reduced forms of iron-tetraphenylporphyrins.

References

1. Gray, H. B., & Winkler, J. R. (2003). Heme protein dynamics: Electron tunneling and redox triggered

folding. In K. M. Kadish, K. M. Smith & G. Guilard (Eds.), *The porphyrin handbook* (Vol. 11, pp. 51–75). Amsterdam: Academic Press.
2. Kobayashi, N. (2010). Meso-azaporphyrins and their analogues. In K. M. Kadish, K. M. Smith & G. Guilard (Eds.), *The porphyrin handbook* (Vol. 2, pp. 301–362). New Jersey: World Scientific Publishing Co.
3. Malinowski, T. (2000). Porphyrin-based electrochemical sensors. In K. M. Kadish, K. M. Smith & G. Guilard (Eds.), *The porphyrin handbook* (Vol. 6, pp. 231–256). San Diego: Academic Press.
4. Gurinovich, G. P., Gurinovich, I. F., Ivashin, N. V., Sinyakov, G. N., Shulga, A. M., Terekhov, S. N., Filatov, I. V., & Dziliński, K. (1988). Electronic structure of metalloporphyrin π-anions. *J. Mol. Struct.*, *172*, 317–343. DOI: 10.1016/0022-2860(88)87026-1.
5. Fukuzumi, S. (2003) Electron transfer chemistry of porphyrins and metalloporphyrins. In K. M. Kadish, K. M. Smith & G. Guilard (Eds.), *The porphyrin handbook* (Vol. 8, pp. 115–151). Amsterdam: Academic Press.
6. Yamaguchi, K., & Morishima, I. (1992). Low-valent iron porphyrins. NMR evidence for π-anion-radical character in two-electron-reduced iron(III) meso- or β-pyrrole-substituted porphyrins. *Inorg. Chem.*, *31*, 3216–3222. DOI: 10.1021/ic00041a010.
7. Collman, J. P., Hoard, J. L., Kim, N., Lang, G., & Reed, C. A. (1975). Synthesis, stereochemistry, and structure-related properties of α, β, γ, δ-tetraphenylporphinatoiron(II). *J. Am. Chem. Soc.*, *97*, 2676–2681. DOI: 10.1021/ja00843a015.
8. Hu, Ch., Noll, B. C., Schultz, C. E., & Scheidt, W. R. (2007). Four-coordinate iron(II) porphyrinates: Electronic configuration change by intermolecular interaction. *Inorg. Chem*., *46*, 619–621. DOI: 10.1021/ic0620182.
9. Tanaka, K., Elkaim, E., Li, L., Jue, Z. N., Coopens, P., & Landrum, J. (1986). Electron density studies of porphyrins and phthalocyanines. IV. Electron density distribution in crystals of (meso-tetraphenylporphinato)iron(II). *J. Chem. Phys*., *84*, 6969–6978. DOI: 10.1063/1.450617.
10. McGarvey, B. R. (1988). Theory of the temperature dependence of the NMR shift of intermediate spin (S = 1) four-coordinate ferrous porphyrins. *Inorg. Chem*., *27*, 4691–4698. DOI: 10.1021/ic00299a004.
11. Coppens, P., & Li, L. (1984). Electron density studies of porphyrins and phthalocyanines. III. The electronic ground state of iron(II)phthalocyanine. *J. Chem. Phys*., *81*, 1983–1993. DOI: 10.1063/1.447821.
12. Wei, L., She, Y., Yu, Y., Yao, X., & Zhang, S. (2012). Substituent effects on geometric and electronic properties of iron tetraphenylporphyrin: a DFT investigation. *J. Mol. Model.*, *18*, 2483–2491. DOI: 10.1007/s00894-011-1279-x.
13. Liao, M. S., & Scheiner, S. (2002). Electronic structure and bonding in unligated and ligated Fe(II) porphyrins. *J. Chem. Phys. 116*, 3635–3644. DOI: 10.1063/1.1447902.
14. Reed, C. A., Mashiko, T., Scheidt, W. R., Spartalian, K., & Lang, G. (1980). High-spin iron(II) in the porphyrin plane. Structural characterization of (meso-tetraphenylporphynato)bis(tetrahydofuran)iron(II). *J. Am. Chem. Soc*., *102*, 2302–2306. DOI: 10.1021/ja00527a028.
15. Lecomtr, C., Blessing, R. H., Coppens, P., & Tabard, A. (1986). Electron-density studies of porphyrins and phthalocyanines. Electronic ground state of iron(II) tetraphenylporphyrin bis(tetrahydrofuran). *J. Am. Chem. Soc*., *108*, 6942–6950. DOI: 10.1021/ja00282a019.
16. Kaczmarzyk, T., Jackowski, T., & Dziliński, K. (2007). Spectroscopic characteristics of Fe^{I}-phthalocyanine. *Nukleonika*, *52*, 99–103.
17. Debrunner, P. G. (1989). Mössbauer spectroscopy of iron porphyrins. In A. B. P. Lever & H. B. Gray (Eds.), *Iron porphyrins* (Part III, pp. 140–234). New York: VCH Publishers.
18. Sams, J. R., & Tsin, T. B. (1979). Mössbauer spectroscopy of iron porphyrins. In D. Dolphin (Ed.), *The porphyrins* (Vol. 4, pp. 425–447). New York: Academic Press.
19. Stanek, J., & Dziedzic-Kocurek, K. (2010). Magnetism of ferriprotoporphyrin IX monomers and dimmers. *J. Magn. Magn. Mater*., *332*, 999–1003. DOI: 10.1016/j.jmmm.2009.12.004.
20. Dziedzic-Kocurek, K., Okła, D., & Stanek, J. (2013). Magnetic interactions in frozen solutions of ironporphyrins. *Nukleonika*, *58*, 83–86.
21. Lang, G., & Spartalian, K. (1978). Mössbauer effect study of the magnetic properties of S = 1 ferrous tetraphenylporphyrin. *J. Chem. Phys*., *69*, 5424–5447. DOI: 10.1063/1.436532.
22. Boyd, P. D. W., & Buckingham, R. F. (1979). Paramagnetic anisotropy, average magnetic susceptibility, and electronic structure of intermediate-spin S = 1 (5,10,15,20-tetraphenylporphyrin)iron(II). *Inorg. Chem*., *18*, 3585–3591. DOI: 10.1021/ic50202a059.
23. Zhan, C. G., Nichols, J. A., & Dixon, D. A. (2003). Ionization potential, electron affinity, electronegativity, hardness and electron excitation energy: Molecular properties from Density Functional Theory orbital energy. *J. Phys. Chem. A*, *107*, 4184–4195. DOI: 10.1021/jp0225774.
24. Khandelwal, S. C., & Roebber, J. L. (1975). The photoelectron spectra of tetraphenylporphine and some metallotetraphenylporphyrins. *Chem. Phys. Lett*., *34*, 355–359. DOI: 10.1016/0009-2614(75)85292-4.
25. Chen, H. L., & Ellis, P. E. (1994). Correlation between gas-phase electron affinities, electrode potentials, and catalytic activities of halogenated metalloporphyrins. *J. Am. Chem. Soc*., *116*, 1086–1089. DOI: 10.1021/ja00082a034.
26. Scheidt, W. R., & Lee, Y. J. (1987). Recent advances in the stereochemistry of metallotetrapyrroles. *Struct. Bond.*, *64*, 1–70. DOI: 10.1007/BFb0036789.